Microhardness and Wear Behavior of Nanodiamond-Reinforced Nanocomposites for Dental Applications

Rocío Moriche *, Joaquín Artigas-Arnaudas, Bhanu Chetwani, María Sánchez *, Mónica Campo, Margarita GONZALEZ PROLONGO, Joaquín Rams, Silvia González Prolongo, Alejandro Ureña

Posted Date: 27 March 2024

doi: 10.20944/preprints202403.1688.v1

Keywords: nanodiamond/polymer-matrix composite; wear; hardness; photocuring

Article

Microhardness and Wear Behavior of Nanodiamond-Reinforced Nanocomposites for Dental Applications

Rocío Moriche [1,2,*], Joaquín Artigas-Arnaudas [1], Bhanu Chetwani [1], María Sánchez [1,3,*], Mónica Campo [1], Margarita G. Prolongo [4], Joaquín Rams [1,3], Silvia G. Prolongo [1,3] and Alejandro Ureña [1,3]

[1] Materials Science and Engineering Area, Escuela Superior de Ciencias Experimentales y Tecnología, Universidad Rey Juan Carlos, Calle Tulipán s/n, 28933 Móstoles, Madrid, Spain
[2] Dpto. de Física de la Materia Condensada, ICMS, CSIC-Universidad de Sevilla, Apdo. 1065, 41080 Sevilla, Spain
[3] Instituto de Investigación de Tecnologías para la Sostenibilidad, Universidad Rey Juan Carlos, C/Tulipán s/n, 28933 Móstoles, Madrid, Spain
[4] Dpt. Aerospace Materials and Production. E.T.S.I. Aeronáutica y del Espacio, Universidad Politécnica de Madrid. Plaza del Cardenal Cisneros, 3, 28040 Madrid, Spain
* Correspondence: rmoriche@us.es (R.M.); maria.sanchez@urjc.es (M.S.)

Abstract: In polymer-based dental composites, wear is a three-body wear system mainly abrasive, because of the food particles and wear products suspended in the oral cavity, which are transferred to the microcavities of the surface of the replacements. Due to this fact, the incorporation of nanodiamond as reinforcement in these polymer matrix composites, which promotes the creation of a solid lubricant tribofilm surface could be advantageous. When nanodiamond is added in contents of 0.8, 1.6 and 3.2 wt %, an increase in microhardness from 95 up to 420 %, compared to the one of neat BisGMA/TEGDMA, is observed. Additionally, the incorporation of a content of 1.6 wt % is enough to cause a diminution of ~78 % in the friction coefficient and a reduction of the specific wear rate and Archard's coefficient of ~50 %. Nevertheless, the addition of relatively high contents reduces the effectiveness of photoinitiation and UV-curing, which is related to the scattering and absorption of UV radiation by ND.

Keywords: nanodiamond/polymer-matrix composite; wear; hardness; photocuring

1. Introduction

Nowadays, resin-based composites (RBCs) are widely used in dentistry for applications as filling materials, restorations, endodontic posts and cores, and adhesives [1]. The most common matrices used for these applications are bisphenol A-glycidyl methacrylate (BisGMA), urethane dimethacrylate (UDMA) and triethylene glycol dimethacrylate (TEGDMA) [2–4]. Although they have been used for 50 years, enhancement of mechanical properties and reduction of shrinkage needs to be further investigated [5].

For this reason, dental polymer-matrix composites with high wear resistance are a current challenge, which is also one of the key properties in long-term restorations [6]. Nevertheless, in addition, the restoration part has to prevent wear of the antagonist tooth that can affect functionalities of the natural tooth [7].

The use of certain ceramic nanoparticles [8], such as TiO_2, ZrO_2, Al_2O_3, and SiC, and graphene nanoplatelets [9], as fillers have demonstrated to enhance tribological properties due to the increase of hardness, diminution of coefficient of friction or the formation of a transfer film between the material and the counterpart. These nanocomposite materials are also potential candidates to prevent

 doi:10.20944/preprints202403.1688.v1

contact between erosive agents and the dental surface, i.e. to prevent dental erosion, by creating a physical barrier [10,11]. Different authors, such as M. Santos *et al.* [12], have also corroborated that commercial dental composites incorporating reinforcements with smaller size distributions show lower coefficients of friction, what leads to lower contact forces and, as consequence, lower wear rates.

Additionally, the use of nanoreinforcements instead of microfillers, due to their higher specific surface area, contributes to an enhancement of mechanical properties and hardness because of the increase in the contact between the polymeric matrix and the nanoparticles [13].

Particularly, nanodiamond (ND) particles have been previously studied to develop new formulations of lubricant colloids [14,15], showing promising results related to wear behavior of sliding parts [16]. A. Golchin et al. [1] have also obtained wear resistance improvements in ultra-high molecular weight polyethylene (UHMWPE) reinforced with ND. Furthermore, Y. Haleem et al. [18] corroborated that the addition of ND (0.5-2 wt %) as nanoreinforcement of epoxy matrixes causes an increase in the fracture toughness and fracture energy.

In this work, the potential use of ND as nanoreinforcement in dental polymer composites is analyzed. A study of the microhardness and wear behavior is carried out as function of ND content (0.6, 1.2 and 3.2 wt %). Additionally, the influence of the addition of ND on UV-curing is also studied to stablish the limit contents to ensure functionality. In order to compare the benefits with a micrometric filler usually used in dental composites, SiO2 microparticles was also used in the study.

2. Materials and Methods

2.1. Materials

The polymeric matrix used in nanocomposites was a Bisphenol A bis(2-hydroxyl-3-methacryloxypropyl) ether (BisGMA) and triethylene glycol dimethacrylate (TEGDMA) in a 50:50 ratio, both purchased from *Esschem Europe*. As reducing agent, camphorquinona (CQ) was added in a content of 0.7 wt%, which is activated at a UV wavelength range of 400-500 nm (maximum peak at 468 nm) and was also provided by *Esschem Europe*. With the aim of promoting polymerization, dimethylaminoethylmethacrylate (DMAEM), *Esschem Europe*, was used in a 0.32 wt%.

Diamond nanopowder (ND) with a particle size lower than 10 nm and a purity ≥ 97%, supplied by *Sigma-Aldrich*, was used as nanofiller. Micrometric silica (SiO_2) powder with a specific surface area (BET) of 200 ± 25 m^2/g from *Scharlab* was also used as reinforcement for comparison.

2.2. Methods

2.2.1. Nanocomposites Manufacturing

Dispersion of the reinforcement was carried out by probe sonication (*Hielscher UP400S*). Nanocomposites with ND contents of 0.8, 1.6 and 3.2 wt % and SiO_2 contents of 1.6, 3.2, 10, and 25 wt % were respectively prepared. Contents were selected based on processability of nanocomposites to ensure their quality. Sonication was applied for 30 minutes with a power amplitude of 50% and a cycle of 0.5 seconds. Once dispersion was fulfilled, the mixture was cured with a UV lamp *RADII PLUS* + for 8 minutes.

2.2.2. Microhardness and Wear Characterization

Vickers microhardness tests were performed following the ASTM E 92-82 in a *Micro Hardness Tester Shimadzu*. The applied load was 980.7 mN and the maximum load was maintained for 30 s. At least, 5 measurements were carried out for each condition. Density of materials was measured by Archimedes' method.

Tribological tests were carried out in a *MicroTest MT400* machine using a pin-on-disk configuration, in dry conditions and with the same environmental conditions. An alumina ball with a diameter of 6 mm was used as counterpart, applied load was 10 N and the track diameter was 10 mm. Sliding was performed until completing a total distance of 500 m with a speed of 200 rpm. Five wear tests were made for each material, and the average value and standard deviation were

 doi:10.20944/preprints202403.1688.v1

determined. The tribological behaviour was evaluated by measuring the volume loss, friction coefficient (μ) and wear rate (Q) of the nanocomposites. The wear testing machine continuously recorded the friction coefficient.

Specific wear rate (Q) was calculated from the mass loss (m), the applied load (W), density (ρ) and total length (L) following the equation 1:

$$Q = \frac{m}{W\rho L} \quad (1)$$

Additionally, the Archard's coefficient (K) was obtained from the empirical Archard's law (equation 2):

$$Q = K\frac{W}{H} \quad (2)$$

where H is the hardness of the tested material.

The samples surface preparation was performed prior to the wear tests. They were ground with different emery papers to obtain a similar surface roughness that would not influence the wear properties. The average roughness of the samples, determined by a profilometer *Mitutoyo SJ-301 Surftest*, was 0.37 ± 0.05 μm.

Three-dimensional profiles of the wear tracks were analyzed by using optical profilometry (*Zeta 20 model* from *KLA-Tencor*). Scanning electron microscopy (SEM), *Hitachi S-2400 N*, was also used to evaluate the morphology and the wear mechanisms of nanocomposites.

2.2.3. UV-Curing Characterization

Based on the obtained results of the evaluation of microhardness and wear behavior of ND-based nanocomposites, a nanoindentation profile was conducted in 3.2 wt% reinforced ones in order to evaluate UV-curing. The profile was generated through the polished cross-section. The distance between adjacent nanoindentations was 25 μm and the maximum applied load was 100 mN with a holding time of 10 s.

Glass transition temperature was measured in a specimen with representative thickness by differential scanning calorimetry (DSC) in a *Mettler Toledo mod.822e*. The temperature range of thermal scans was from 10 up to 200 °C with a heating rate of 20 °C/min, under nitrogen atmosphere.

Fourier-transform infrared spectroscopy (FTIR) was used to analyze differences in UV-curing through thickness. Measurements was carried out in a *Nicolet iN10 MX* infrared microscope with a Ge attenuated total reflection (ATR). Five FTIR spectra between 700-4000 cm^{-1} wavelengths were recorded along 1500 μm from the surface of the nanocomposite where UV light was irradiated.

3. Results

3.1. Microhardness of ND-Nanocomposites

The addition of ND to the polymeric matrix is thought to contribute to mechanical properties in order to replace current micrometric reinforcement by nanometric ones to enhance polishing and mechanical and tribological behavior. Figure 1 shows Vickers microhardness (HV0.1) of ND-based nanocomposites as well as SiO_2-based nanocomposites, for comparison, as a function of reinforcement content. The values of microhardness of commercially available composite materials, measured using the same method, have been also added for comparison. Reinforcement contents in these commercial composite materials, with particle sizes from the nanometer scale up to 50 μm in some cases, ranges from 60 up to 80 wt %.

The incorporation of 0.8 wt % of ND causes an increase in microhardness of ~ 95 %, while the quantity needed to reach similar microhardness for micrometric SiO_2 reinforcement is above 3.2 wt%. Moreover, microhardness increases by ~ 420 % in the case of using ND with a content of 3.2 wt %; this value has not been reached with SiO_2 even with concentrations up to 25 wt %. Additionally, it is important to point out that the microhardness of composites reinforced with 10 wt % of micrometric

 doi:10.20944/preprints202403.1688.v1

SiO_2, which is 23.7 ± 0.4, is still lower than the one of nanocomposites filled with 1.6 wt % of ND, being 27.7 ± 3.4.

If these values are compared with the microhardness of commercial dental composites, nanocomposites reinforced with contents as low as 0.8 wt% present values above some of the mentioned commercially available composites. Taking into account that other reinforcements used to achieve multifunctionality in dental composites are included in the commercial ones and the fact that the levels of filler ratios in the polymeric matrix are considerably higher, the obtained results evidence the potential application of ND as nanoreinforcement to be used in dental composite materials. The low contents of ND needed are also advantageous to new manufacturing methods, such as 3D printing, where low reinforcements contents are required to keep the composites flowable and avoid different curing degrees [6].

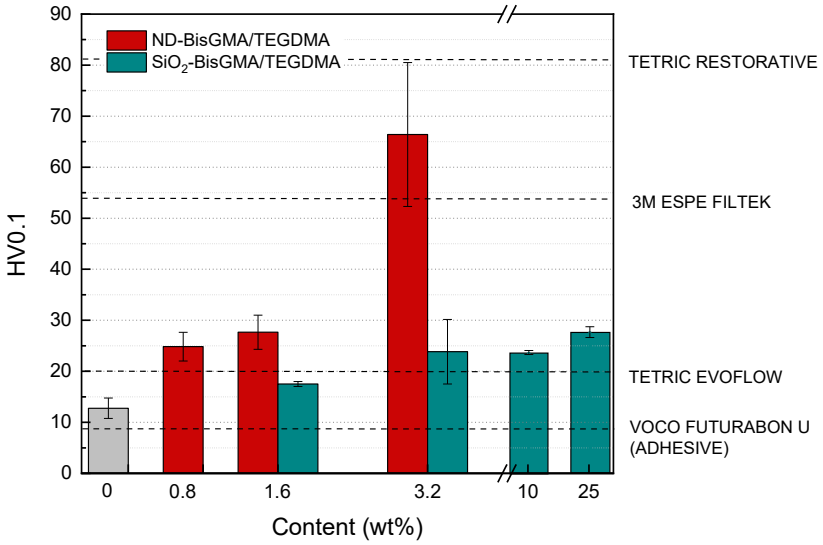

Figure 1. Vickers microhardness of ND-reinforced nanocomposites and SiO_2- reinforced nanocomposites; and commercial *Voco Futurabond U*, *Tetric Evoflow*, *3M ESPE Filtek* and *Tetric Restorative*.

3.2. Wear Behavior of ND-Nanocomposites

Figure 2 shows the evolution of the coefficient of friction (μ) during the test (Figure 2a) and the average μ, calculated as the average value in the stabilized region (Figure 2b). Results show that stabilization occurs at longer times as the NDs content increases, except in the case of 1.6 wt %. The friction coefficient diminishes ~24 % with a content of 0.8 wt %, and considerably reduced ~78 % when the ND content was duplicated, i.e. 1.6 %. When using a ND content of 3.2 wt %, an increase in friction coefficient is observed but it still is lower than the BisGMA/TEGDMA one (0.57 ± 0.06). The reasons are related to the increase in microhardness and wear mechanisms that takes places, which will be discussed later.

 doi:10.20944/preprints202403.1688.v1

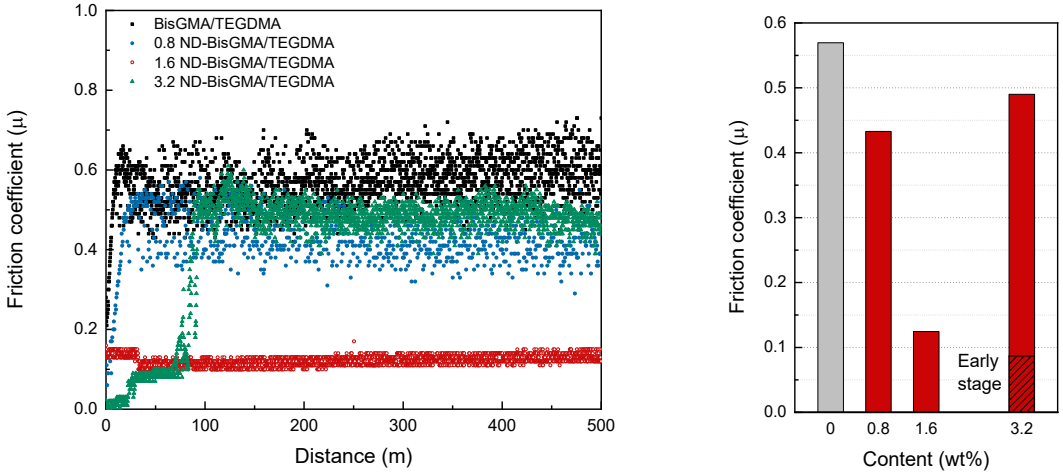

(**a**) (**b**)

Figure 2. Friction coefficient (μ) of ND-reinforced nanocomposites (**a**) time dependence and (**b**) friction coefficient values.

A previously published work reported by E. Koumoulos et al. [19] shows that the friction coefficient, calculated from nanoscratch tests, of epoxy-matrix nanocomposites incorporating ND as reinforcement diminishes as the NDs content increases from 0.4 up to 5.0 wt %. The friction coefficient (μ) value reduced from ~0.45 down to ~0.40, i.e. ~11%; which elucidates the lubricant effect created by detached ND.

The volume loss of ND-reinforced nanocomposites and SiO_2-reinforced composites depending on the filler content is plotted in Figure 3a and Figure 3b, respectively. Although the volume loss of nanocomposites reinforced with a 0.8 wt % of ND experienced an increase, when the content is augmented up to 1.6 wt %, the volume loss decreased by near 50 %. This fact is attributed to the effect that a certain level of concentration of ND induces autolubricity in nanocomposites. The mechanism taking place is that ND nanoparticles favor sliding between the three bodies, i.e. nanocomposite, ND and alumina ball. When ND nanoparticles detach due to wear, they act as bearing, promoting, consequently, a lubricity effect [20] and giving rise to the formation of a film, acting as a lubricating layer (tribofilm) [21]. This proposed mechanism has been previously published by A.M. Tortora *et al.* [15] and M. Ivanov *et al*. [14]. Additionally, the increase in microhardness also contributes to the enhancement observed in wear behavior [17].

In contrast to the reduction observed for ND-reinforced nanocomposites, when micrometric SiO_2 is added as filler, the volume loss is considerably higher, being twice the one of the BisGMA/TEGDMA polymer for a content of 3.2 wt % and 4 times higher in the case of adding a concentration of 25 wt %. In this case, detached SiO_2 microparticles act as abrasive body between the counterpart and the surface of the composite causing higher wear and, therefore, higher volume loss [22]. The increase in wear resistance by incorporation of inorganic reinforcements has been attributed to the enhancement in hardness [23], but once these microparticles are detached, they can get involved in a three-body wear system.

 doi:10.20944/preprints202403.1688.v1

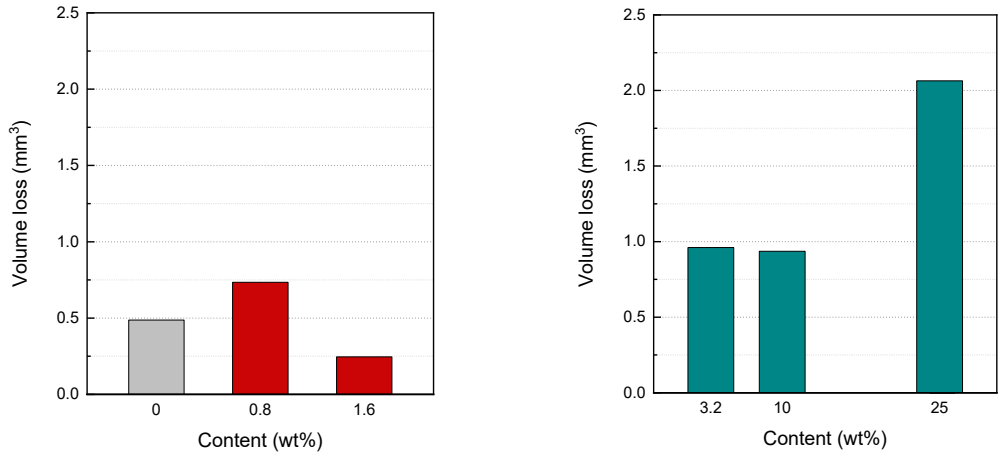

(**a**) (**b**)

Figure 3. Friction coefficient (μ) of ND-reinforced nanocomposites (**a**) time dependence and (**b**) friction coefficient values.

Figure 4 shows specific wear rates of the composites for the tested condition. The specific wear rate of BisGMA/TEGDMA is near 10^{-4} mm^3/Nm and the Archard's coefficient is $2.6 \cdot 10^5$. H. Chadda *et al.* [24] obtained a specific wear rate for non-reinforced BisGMA/TEGMA at a load of 25 N of the same order of magnitude. With the addition of 0.8 wt %, the specific wear rate as well as the Archard's coefficient increases, which is in accordance with the results discussed above. In contrast, a content of 1.6 wt %, due to the formation of the solid lubricant tribofilm, induces a reduction in both specific wear rate and Archard's coefficient of ~50 %. The contrary happens when micrometric SiO_2 is used as reinforcement, an increase in specific wear rate and Archard's coefficient occurs, due to the abrasion of the detached SiO_2 microparticles.

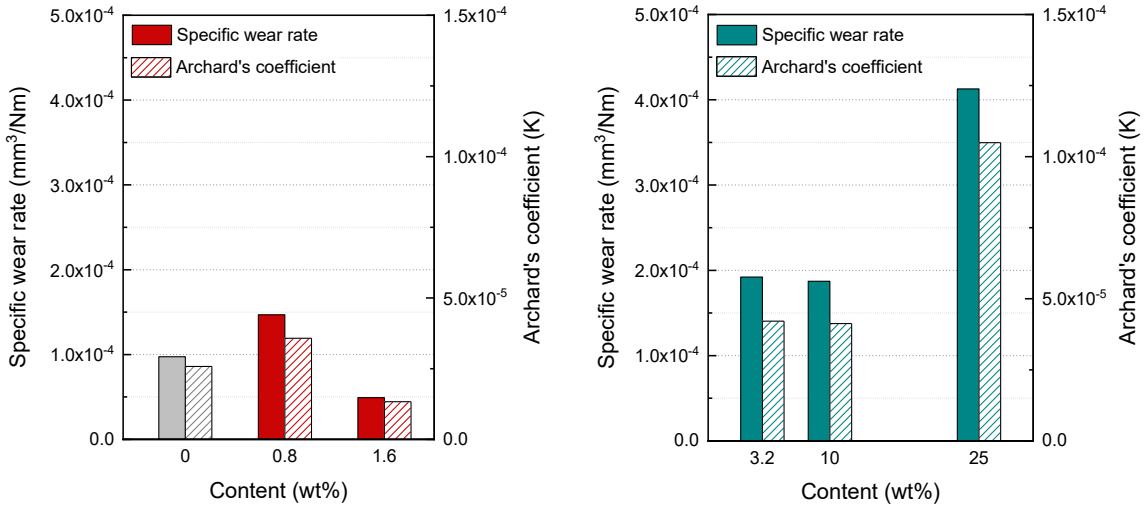

(**a**) (**b**)

Figure 4. Friction coefficient (μ) of ND-reinforced nanocomposites (**a**) time dependence and (**b**) friction coefficient values.

 doi:10.20944/preprints202403.1688.v1

In order to analyze mechanisms taking place, Figure 5 shows representative SEM micrographs of the surfaces of the wear tracks produced by wear. The surface of the BisGMA/TEGDMA wear track (Figures 5a and 5e) shows plowing marks in the direction of the sliding movement of the counterpart, which is significant of micro-cracks propagation along that direction. Additionally, there is accumulation of polymeric material, i.e. pile-up, in the track contour. These two phenomena are representative of a combined abrasive and adhesive wear mechanism. The addition of low contents of ND does not induce appreciable modifications (Figures 5b and 5f), although a slight change in the morphology of the surface of wear track and pile-up is less significant. Initially, detachment of ND/BisGMA/TEGDMA occurs forming the debris. During the ball movement, debris act as a third body [25] as the ND content is not enough to create an effective solid lubricant tribofilm. Additionally, as it will be discussed later (section 3.3), the addition of ND influences photocuring of nanocomposites, as ND acts as UV light scattering center. If debris detached due to wear has not enough ND content to create the mentioned tribofilm, material is torn out [26], creating voids, as the degree of curing slightly diminishes along the thickness.

In contrast, a content of 1.6 wt %, as shown in the previous discussion, considerably changes tribology. Wear is significantly reduced, and wear track is near imperceptible (Figure 5c and 5g). This is due to the effective autolubricant properties of the nanocomposite material already mentioned above, together with the increase in microhardness.

The wear track surface of SiO_2-based composites shows differences, Figures 5d and 5h show SEM micrographs of composites reinforced with 10 wt%, which are representative to define mechanisms. Due to the presence of SiO_2, the accumulation of material in the contour of the wear track is negligible, which is indicative of a significant reduction of adhesive wear and more dominancy of abrasive wear. In this case, detached SiO_2 particles act as abrasive in the three body wear system, not only in micrometric but also in nanometric scale size, as it has been previously reported by J. Abenojar *et al.* [22], L. Zhang *et al.* [9] and Y. Zhao *et al.* [27] in other polymeric matrix composites. Generally, in dental composites, abrasive wear is the most common mechanism, which is originated under plastic conditions and because of the contact of hard particles with a softer surface [28].

In polymer-based dental composites, the usual wear is mainly abrasive, because of the food particles and wear products suspended in the oral cavity, which are transferred to the microcavities of the surface of the replacements [29]. Due to this fact, the creation of the lubricant tribofilm surface could be advantageous.

All the results mentioned above are also in accordance with the morphology and size of wear tracks. Figures 6 and 7 shows representative profilometries of the wear tracks after completing the wear tests, as well as geometrical parameters. In these profilometries, the effect of the addition of 1.6 wt % of ND nanoparticles can be clearly appreciated as the wear is nearly non appreciable (Figure 6c) and the depth is nearly negligible (Figure 7a). It is also important to point out the wider and deeper geometry of wear tracks induced in SiO_2-based composites, significantly higher than that of the ND-based composites with similar Vickers microhardness.

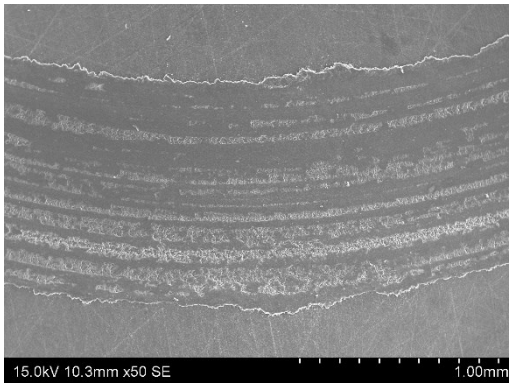

(**a**)

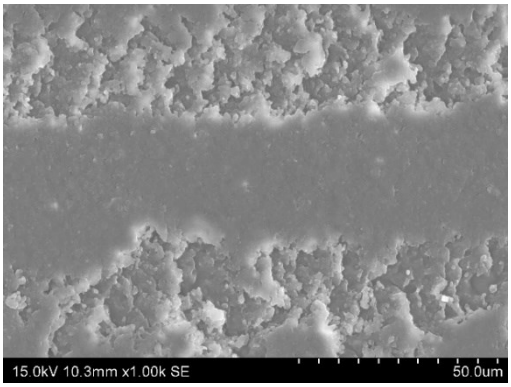

(**e**)

 doi:10.20944/preprints202403.1688.v1

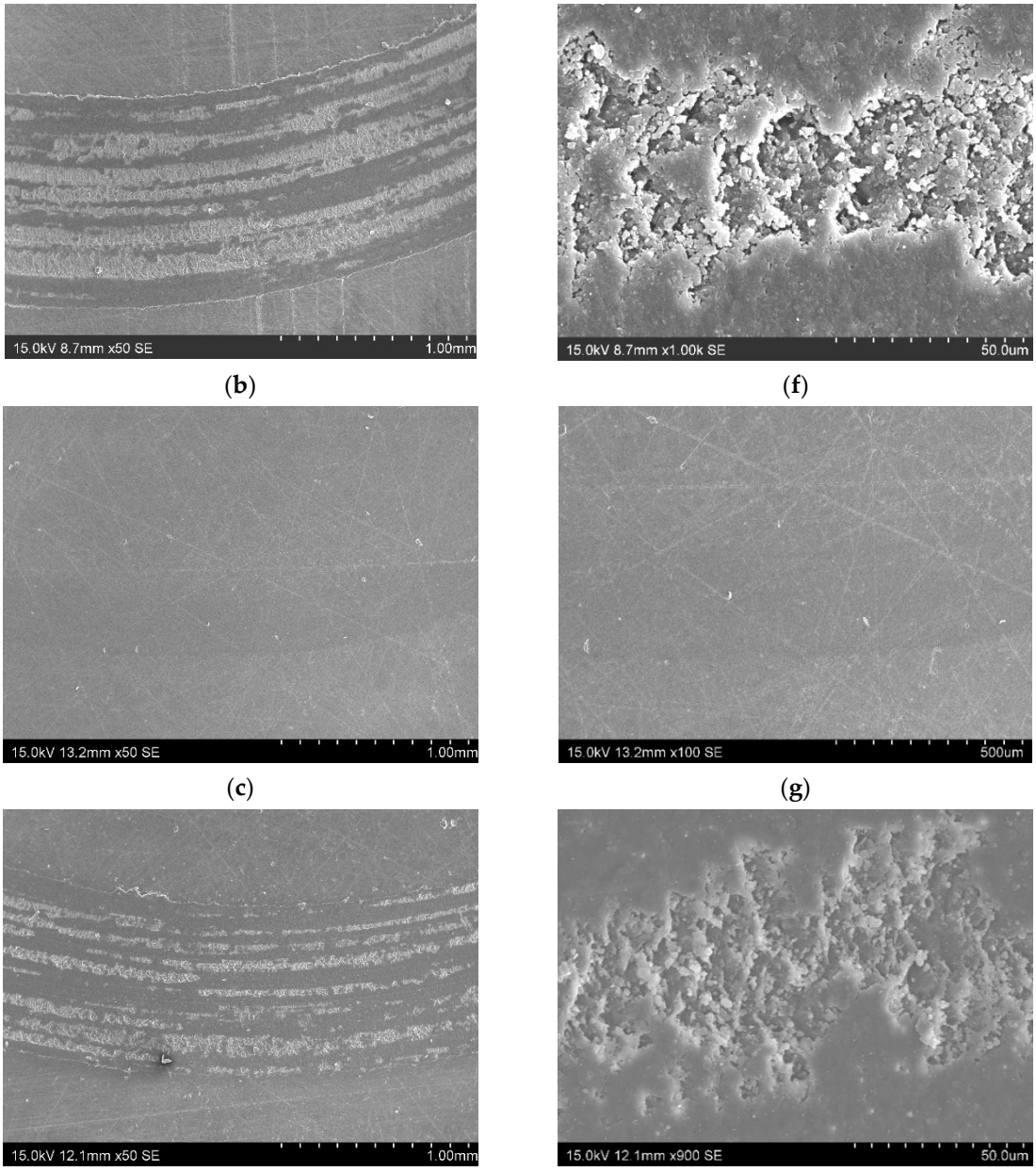

(**b**) (**f**)

(**c**) (**g**)

(**d**) (**h**)

Figure 5. SEM micrographs of wear tracks of (**a**,**e**) BisGMA/TEGDMA; ND-reinforced nanocomposites, (**b**,**f**) 0.8 and (**c**,**g**) 1.6 wt%; and 10SiO_2-reinforced nanocomposites, (**d**,**h**) 10 wt%.

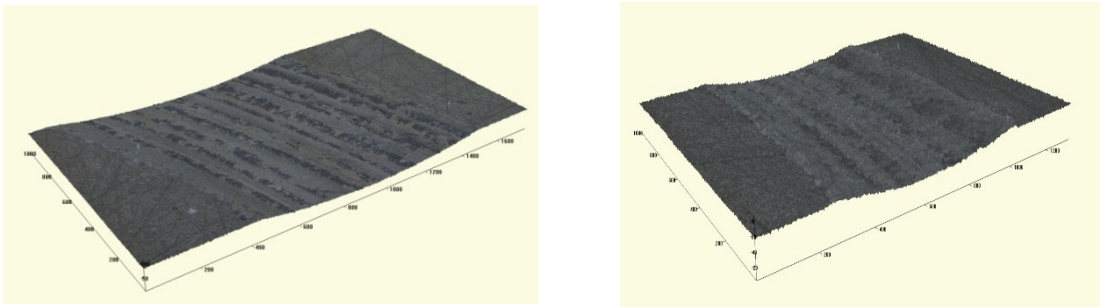

(**a**) (**d**)

 doi:10.20944/preprints202403.1688.v1

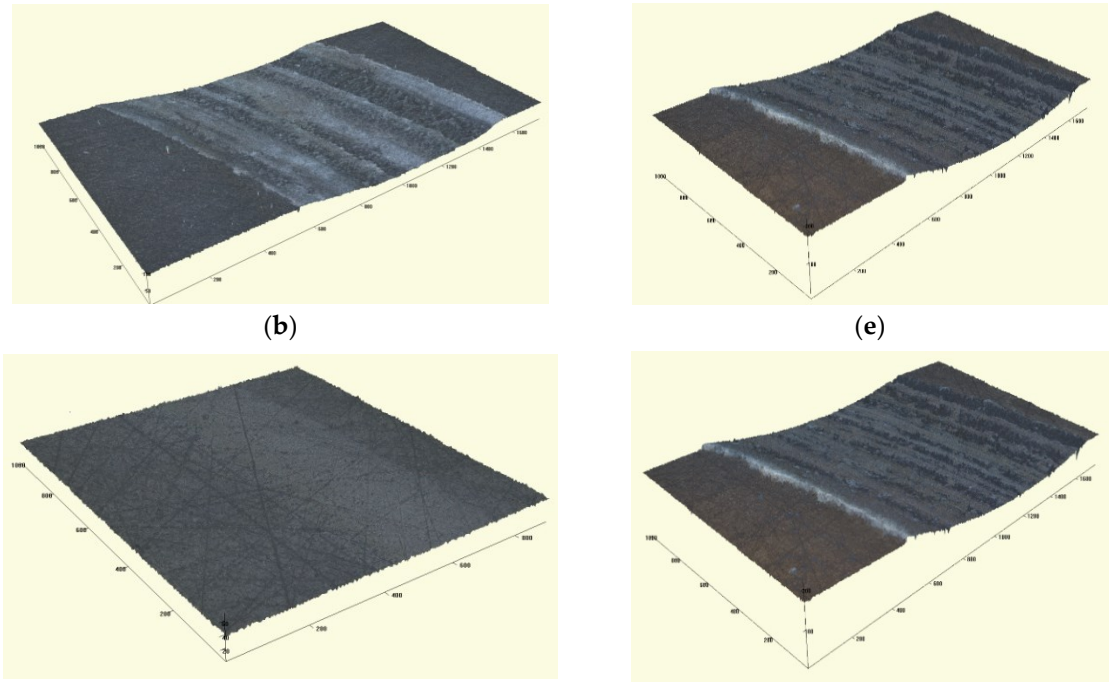

Figure 6. Profilometry of wear tracks of (**a**) BisGMA/TEGDMA; (**b**,**c**) ND-reinforced nanocomposites, (**b**) 0.8 and (**c**) 1.6 wt%; and (**d**-**f**) SiO_2-reinforced nanocomposites, (**d**) 3.2, (**e**) 10, and (**f**) 25 wt %.

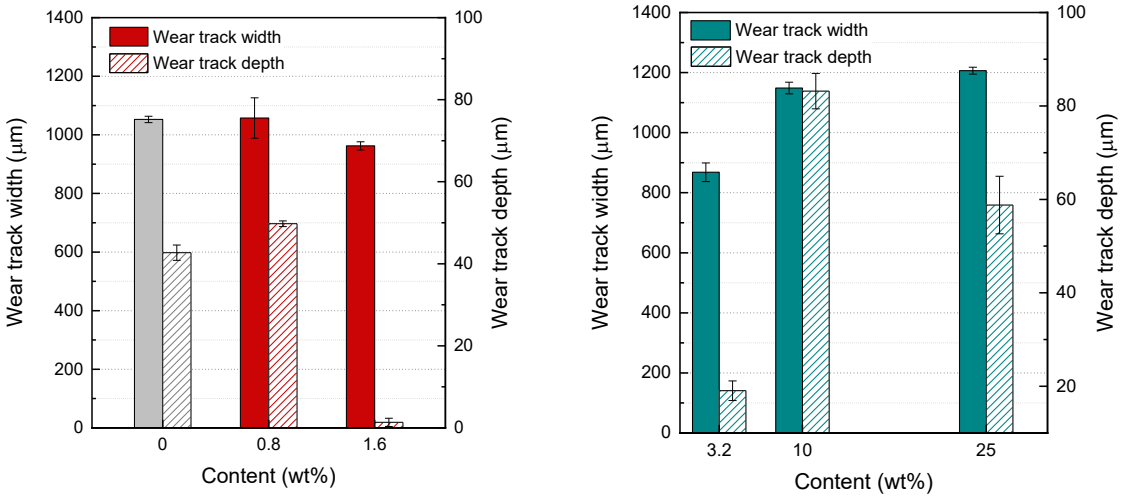

Figure 7. Wear track width and depth of (**a**) ND-reinforced nanocomposites and (**b**) SiO_2 reinforced nanocomposites.

3.3. UV-Curing Analysis of ND-Based Nanocomposites

Due to differences found in wear behavior of 3.2 wt % ND-reinforced nanocomposites, a deep analysis of UV-curing of this composition was carried out with the aim of elucidating the influence of the addition of ND in relatively high contents. Results of additional nanoindentation tests along the cross-section, as well as FTIR and DSC analysis, are shown in Figure 8.

The evolution of the elastic modulus and hardness calculated from nanoindentation profiles curves (Figure 8a) shows a progressive diminution of mechanical properties from the surface of the

 doi:10.20944/preprints202403.1688.v1

nanocomposite with depth. The observed decreased is attributed to differences in UV-curing along the cross-section of the sample. To corroborate this statement, FTIR spectra were recorded depending on the distance to the surface. Figure 8b shows the correspondent spectra. If the peak associated to C=C of methacrylate groups that has not reacted is analyzed, which is located at ~1635 cm^{-1}, it increases as the FTIR spectrum recorded corresponds to a deeper section of the nanocomposites. Thus, the concentration of non-reacted methacrylate groups is higher with increasing depth. This fact is related to the scattering and absorption of UV radiation by ND already observed in nanodiamond hydrosols by A. Vu *et al.* [30], and has been also detected with other reinforcements for dental applications, as reported by L. Rodrigues de Menezes *et al.* [31], what reduces the effectiveness of photoinitiation and the creation of the radical species.

To solve these heterogeneities, different UV-curing times (8, 16, 24, and 32 min), although they may be not effective to be applicable in cases of in-situ polimerization. Figure 8c shows glass transition temperature (T_g) of BisGMA/TEGDMA and ND-reinforced nanocomposites for UV-curing times of 8, 16, 24, and 32 min. The exposure to UV light for longer times makes possible the increment of T_g values up to the same value of the neat BisGMA/TEGDMA matrix. Although ND should act as steric blockers of polymeric chains movement resulting in an increase of T_g, because of the scattering and absorption of UV-radiation, the expected increase is not achieved.

R. Odermatt *et al.* [32] have also reported lower degrees of curing when using nano- and micrometric bioglass as fillers. After 24 h, the degree of curing in both cases is near 20 % lower than the one of the polymeric matrix. But after 28 days, the achieved degree of curing increased reaching the same of the non-reinforced polymer.

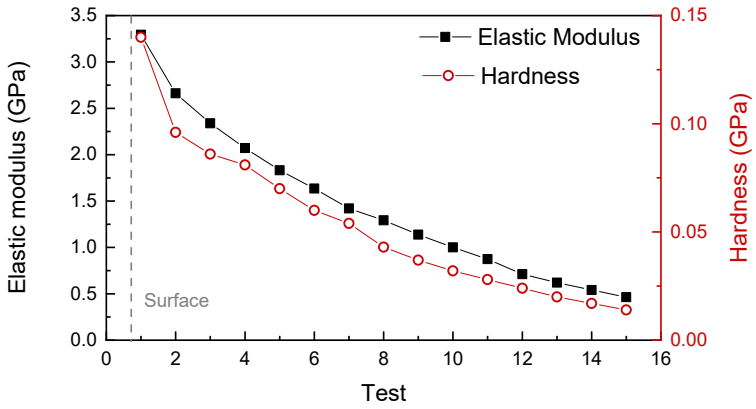

(**a**)

 doi:10.20944/preprints202403.1688.v1

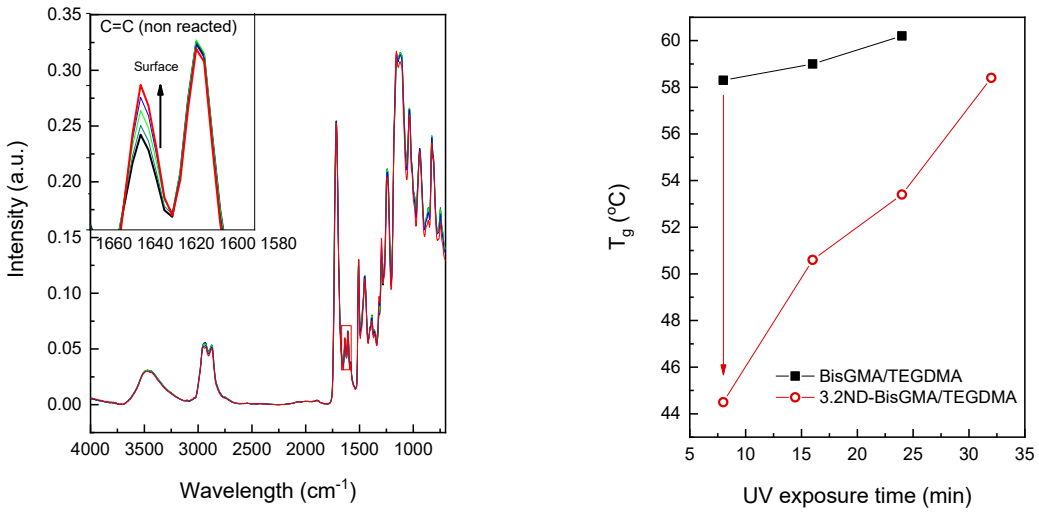

(**b**) (**c**)

Figure 8. Analysis of UV-curing of 3.2 wt% ND-reinforced nanocomposites: (**a**) elastic modulus and hardness profiles, and (**b**) FTIR as a function of the distance to the surface; and (**c**) glass transition temperature (T_g).

4. Conclusions

The enhancement in micromechanical and wear behavior of ND-reinforced BisGMA/TEGDMA nanocomposites has been analysed. An addition of 1.6 and 3.2 wt % of ND to the polymeric matrix results in microhardness values in the range of the ones of commercially available dental composites. But, the low contents of ND needed to achieve these values are more advantageous to new manufacturing methods, such as 3D printing, where low reinforcements contents are required to keep the composites flowable and avoid different curing degrees. The enhanced tribological properties are due to the creation of a lubricant tribofilm, which significantly inhibits progressive wear.

Although ND has been demonstrated to enhance mechanical and tribological properties, relatively high contents, i.e. 3.2 wt %, reduces the effectiveness of photoinitiation, UV-curing, related to the scattering and absorption of UV radiation by ND. This phenomenon could be solved by increasing UV exposure time.

Author Contributions: Conceptualization, J.R. and A.U.; methodology, R.M., M.S., M.C., M.G.P., S.G.P., J.R. and A.U.; formal analysis, R.M., J.A., M.G.P. and S.G.P.; investigation, R.M., J.A., B.C. and M.G.P.; resources, M.S., J.R., S.G.P. and A.U.; data curation, R.M., J.A. and B.C.; writing—original draft preparation, R.M.; writing—review and editing, R.M., M.S., M.C., J.R., S.G.P. and A.U.; supervision, M.S., M.C., J.R., S.G.P. and A.U.; project administration, M.S. and A.U.; funding acquisition, M.S. and A.U.

Funding: This work was supported by the Agencia Estatal de Investigación of Spanish Government (MULTISENS PID2022-136636OB-I00).

Institutional Review Board Statement: Not applicable.

Informed Consent Statement: Not applicable.

Data Availability Statement: All data are contained within the article.

Conflicts of Interest: The authors declare no conflicts of interest.

References

1. Pirmoradian M.; Hooshmand T.; Jafari-Semnani S.; Fadavi F. Degree of conversion and microhardness of bulk-fill dental composites polymerized by LED and QTH light curing units. *J Oral Biosci* **2020**, 62, 107–113. https://doi.org/10.1016/j.job.2019.12.004.
2. Parasher A.; Ginjupalli K.; Somayaji K.; Kabbinale P. Comparative evaluation of the depth of cure and surface roughness of bulk-fill composites: An in vitro study. *Dent Med Probl* **2020**, 57, 39–44. https://doi.org/10.17219/dmp/113003.
3. Aljabo A.; Abou Neel E.A.; Knowles J.C.; Young A.M. Development of dental composites with reactive fillers that promote precipitation of antibacterial-hydroxyapatite layers. *Mater Sci Eng C* **2016**, 60, 285–92. https://doi.org/10.1016/j.msec.2015.11.047.
4. Ender A.; Bienz S.; Mörmann W.; Mehl A.; Attin T.; Stawarczyk B.; et al. Marginal adaptation , fracture load and macroscopic failure mode of adhesively luted PMMA-based CAD / CAM inlays. *Dent Mater* **2015**, 32, 1–8. https://doi.org/10.1016/j.dental.2015.11.009.
5. Zhang X.; Zhang J.; Zhang T.; Yao S.; Wang Z.; Zhou C.; Wu J. Novel low-shrinkage dental resin containing microcapsules with antibacterial and self-healing properties. *J Mech Behav Biomed Mater* **2023**, 148, 106212. https://doi.org/10.1016/j.jmbbm.2023.106212.
6. Kessler A.; Reymus M.; Hickel R.; Kunzelmann K.H. Three-body wear of 3D printed temporary materials. *Dent Mater* **2019**, 35, 1805–1812. https://doi.org/10.1016/j.dental.2019.10.005.
7. Branco A.C.; Silva R.; Santos T.; Jorge H.; Rodrigues A.R.; Fernandes R.; et al. Suitability of 3D printed pieces of nanocrystalline zirconia for dental applications. *Dent Mater* **2020**, 36, 442–455. https://doi.org/10.1016/j.dental.2020.01.006.
8. Li G.; Qi H.; Zhang G.; Zhao F.; Wang T.; Wang Q. Significant friction and wear reduction by assembling two individual PEEK composites with specific functionalities. *Mater Des* **2017**, 116, 152–159. https://doi.org/10.1016/j.matdes.2016.11.100.
9. Zhang L.; Zhang G.; Chang L.; Wetzel B.; Jim B.; Wang Q. Distinct tribological mechanisms of silica nanoparticles in epoxy composites reinforced with carbon nanotubes, carbon fibers and glass fibers. *Tribol Int* **2016**, 104, 225–236. https://doi.org/10.1016/j.triboint.2016.09.001.
10. Tereza G.P.G.; de Oliveira G.C.; de Andrade Moreira Machado M.A.; de Oliveira T.M.; da Silva T.C.; Rios D. Influence of removing excess of resin-based materials applied to eroded enamel on the resistance to erosive challenge. *J Dent* **2016**, 47, 49–54. https://doi.org/10.1016/j.jdent.2016.02.004.
11. Hasselkvist A.; Johansson A.; Johansson A.K. A 4 year prospective longitudinal study of progression of dental erosion associated to lifestyle in 13–14 year-old Swedish adolescents. J Dent **2016**, 47, 55–62. https://doi.org/10.1016/j.jdent.2016.02.002.
12. Santos M.; Coelho A.S.; Paula A.B.; Marto C.M.; Amaro I.; Saraiva J.; et al. Mechanical and tribological characterization of a dental ceromer. *J Funct Biomater* **2020**, 11, 1–15. https://doi.org/10.3390/jfb11010011.
13. Buldur M.; Sirin Karaarslan E. Microhardness of glass carbomer and high-viscous glass Ionomer cement in different thickness and thermo-light curing durations after thermocycling aging. *BMC Oral Health* **2019**, 19, 1–13. https://doi.org/10.1186/s12903-019-0973-4.
14. Ivanov M.; Shenderova O. Nanodiamond-based nanolubricants for motor oils. *Curr Opin Solid State Mater Sci* **2017**, 21, 17–24. https://doi.org/10.1016/j.cossms.2016.07.003.
15. Tortora A.M.; Halenahally Veeregowda D. Effects of two sliding motions on the superlubricity and wear of self-mated bearing steel lubricated by aqueous glycerol with and without nanodiamonds. *Wear* **2017**, 386–387, 173–178. https://doi.org/10.1016/j.wear.2017.06.015.
16. Pan F.; Khan M.; Tiehu L.; Javed E.; Hussain A.; Zada A.; Alei D.; Wahab Z. Effect of nanodiamond particles on the structure, mechanical, and thermal properties of polymer embedded ND/PMMA composites. *J Polym Eng* **2022**, 42, 795-807. https://doi.org/10.1515/polyeng-2022-0012.
17. Golchin A.; Villain A.; Emami N. Tribological behaviour of nanodiamond reinforced UHMWPE in water-lubricated contacts. *Tribol Int* **2017**, 110, 195–200. https://doi.org/10.1016/j.triboint.2017.01.016.
18. Haleem Y.A.; Song P.; Liu D.; Wang C.; Gan W.; Saleem M.F.; et al. The effect of high concentration and small size of nanodiamonds on the strength of interface and fracture properties in epoxy nanocomposite. *Mater* **2016**, 9, 507. https://doi.org/10.3390/ma9070507.
19. Koumoulos E.P.; Jagadale P.; Lorenzi A.; Tagliaferro A.; Charitidis C.A. Evaluation of surface properties of epoxy-nanodiamonds composites. *Compos Part B: Eng* **2015**, 80, 27–36. https://doi.org/10.1016/j.compositesb.2015.05.036.
20. Chen Z.; Liu Y.; Luo J. Superlubricity of nanodiamonds glycerol colloidal solution between steel surfaces. *Colloids Surf A: Physicochem Eng* **2016**, 489, 400–406. https://doi.org/10.1016/j.colsurfa.2015.10.062.
21. Guo L.; Qi H.; Zhang G.; Wang T.; Wang Q. Distinct tribological mechanisms of various oxide nanoparticles added in PEEK composite reinforced with carbon fibers. *Compos Part A: Appl S* **2017**, 97, 19–30. https://doi.org/10.1016/j.compositesa.2017.03.003.
22. Abenojar J.; Tutor J.; Ballesteros Y.; del Real J.C.; Martínez M.A. Erosion-wear, mechanical and thermal properties of silica filled epoxy nanocomposites. *Compos Part B: Eng* **2017**, 120, 42–53.

23. Zhang X.; Wang H.; Liu Z.; Zhu Y.; Wu S.; Wang C.; et al. Fabrication of durable fluorine-free superhydrophobic polyethersulfone (PES) composite coating enhanced by assembled MMT-SiO2 nanoparticles. *Appl Surf Sci* **2017**, 396, 1580–1588. https://doi.org/10.1016/j.apsusc.2016.11.217.
24. Chadda H.; Satapathy B.K.; Patnaik A.; Ray A.R. Mechanistic interpretations of fracture toughness and correlations to wear behavior of hydroxyapatite and silica/hydroxyapatite filled bis-GMA/TEGDMA micro/hybrid dental restorative composites. *Compos Part B: Eng* **2017**, 130, 132–146. https://doi.org/10.1016/j.compositesb.2017.07.069.
25. Campo M.; Jiménez-Suárez A.; Ureña A. Effect of type, percentage and dispersion method of multi-walled carbon nanotubes on tribological properties of epoxy composites. *Wear* **2015**, 324–325, 100–108. https://doi.org/10.1016/j.wear.2014.12.013.
26. Campo M.; Jiménez-Suárez A.; Ureña A. Tribological properties of different types of graphene nanoplatelets as additives for the epoxy resin. *Appl Sci* **2020**, 10, 4363. https://doi.org/10.3390/app10124363.
27. Zhao Y.; Qi X.; Dong Y.; Ma J.; Zhang Q.; Song L.; et al. Mechanical, thermal and tribological properties of polyimide/nano-SiO2 composites synthesized using an in-situ polymerization. *Tribol Int* **2016**, 103, 599–608. https://doi.org/10.1016/j.triboint.2016.08.018.
28. Wendler M.; Kaizer M.R.; Belli R.; Lohbauer U.; Zhang Y. Sliding contact wear and subsurface damage of CAD/CAM materials against zirconia. *Dent Mater* **2020**, 36, 387–401. https://doi.org/10.1016/j.dental.2020.01.015.
29. Pieniak D.; Walczak A.; Walczak M.; Przystupa K.; Niewczas A.M. Hardness and wear resistance of dental biomedical nanomaterials in a humid environment with non-stationary temperatures. Mater **2020**, 13, 1255. https://doi.org/10.3390/ma13051255.
30. Vul A.Y.; Eydelman E.D.; Sharonova L.V.; Aleksenskiy A.E.; Konyakhin S.V. Absorption and scattering of light in nanodiamond hydrosols. *Diam Relat Mater* **2011**, 20, 279–284. https://doi.org/10.1016/j.diamond.2011.01.004.
31. Rodrigues de Menezes L.; Oliveira da Silva E. The Use of Montmorillonite Clays as Reinforcing Fillers for Dental Adhesives. *Mater Res* **2016**, 19, 236–242.
32. Odermatt R.; Par M.; Mohn D.; Wiedemeier D.B.; Attin T.; Tauböck T.T. Bioactivity and Physico-Chemical Properties of Dental Composites Functionalized with Nano- vs. Micro-Sized Bioactive Glass. J Clin Med **2020**, 9, 772. https://doi.org/10.3390/jcm9030772.